Catalysis Letters Vol. 103, Nos. 1–2, September 2005 (© 2005)
DOI: 10.1007/s10562-005-6504-8

Characteristics and catalytic properties of alumina–zirconia mixed oxides prepared by a modified Pechini method

Patta Soisuwan[a,b], Dean C. Chambers[c], David L. Trimm[b,c], Okorn Mekasuwandumrong[d], Joongjai Panpranot[a], and Piyasan Praserthdam[a,*]

[a]*Centre of Excellence on Catalysis and Catalytic Reaction Engineering, Department of Chemical Engineering, Faculty of Engineering, Chulalongkorn University, Bangkok, 10330 Thailand*
[b]*School of Chemical Engineering and Industrial Chemistry, University of New South Wales, Sydney, NSW, 2052 Australia*
[c]*CSIRO Petroleum, Private Bag 10, Clayton South, VIC, 3169 Australia*
[d]*Department of Chemical Engineering, Faculty of Engineering and Industrial Technology, Silpakorn University, Nakon Pathom, 73000 Thailand*

Received 22 November 2004; accepted 5 May 2005

A modified Pechini method was used to prepare alumina–zirconia mixed oxides at three different molar ratios. For comparison, pure alumina and pure zirconia were prepared using the same method. The mixed oxides were characterised by the BET method for surface area, X-ray diffraction, CO_2 and NH_3 temperature-programmed desorption. Elimination of 2-propanol was used as a probe reaction to characterise the surface of the mixed oxides. The modified Pechini preparation resulted in a poor acid–base strength of alumina surface resulting in high acetone selectivity where imperfect crystal structure of the tetragonal zirconia favoured high propylene production in 2-propanol elimination at 200 °C.

KEY WORDS: alumina; zirconia; mixed oxide; Pechini method; 2-propanol.

1. Introduction

The sol–gel technique is widely used for preparation of ceramic materials, especially mixed oxides, because lower temperatures are required compared to conventional ceramic mixing processes and it improves dispersion and homogeneity [1]. Different precursors have been used to prepare sol–gel materials, particularly metal alkoxides [2–10] and citric acid (CA) complexes [11–13]. The materials obtained from both processes are quite similar but gel formation is approached under different conditions. Zirconia prepared by the sol–gel method, however, usually possesses low surface area. Recently, it has been reported that solid powders were successfully prepared by the modified Pechini method [14,15], in which CA and ethylene glycol are polymerised around metal ions. In 1963, Pechini *et al.* discovered a preparation method of mixed oxides, which can be applied for ceramic and dielectric materials. Because of homogeneous starting solution producing resin intermediate and then resulting in oxide by ignition, this technique leads to closer combination of mixed oxides, which may enhance strong interaction between metal ions. Moreover, high surface area of solid powders is usually obtained by this method, which could bring about high dispersion of metal loading and consequently high active sites for catalytic reactions [15]. In this study, a modified Pechini method was used to prepare alumina, zirconia and alumina–zirconia mixed oxides. Zirconia toughened alumina is generally employed in ceramic application because of its well-known mechanical property, moreover, recently mixed oxide of zirconia and alumina has been introduced in medical application as a biocompatible nano-composite [16]. In catalytic reaction, zirconia alumina has been used as catalyst and/or support because of its surface property, stability and mechanical property. Modification of the mixed oxide by sulfate is well known and showed very good activity of isomerisation [17]. Zirconia alumina at different ratios was prepared to improve surface properties by well-dispersed sol gel preparation. The effect of Al/Zr ratio on the characteristics and catalytic properties of the alumina–zirconia mixed oxides was investigated by means of nitrogen physisorption (BET), X-ray diffraction (XRD) and CO_2 and NH_3 temperature-programmed desorption (TPD). Elimination reactions of 2-propanol were used to determine the catalytic activity of the oxides.

2. Experimental

2.1. Preparation of alumina–zirconia mixed oxides

Alumina–zirconia mixed oxides were prepared using a modified Pechini method in the same manner as that of [14,15] with Al/Zr molar ratios of 1:3, 2:3, 1:1, and 3:1. For comparison, pure alumina and zirconia were prepared by the same method. Aluminium nitrate [$Al(NO_3)_3 \cdot 9H_2O$] and zirconyl nitrate [$ZrO(NO_3)_2 \cdot xH_2O$] were used as precursors. The nitrate salts

---

[*] To whom correspondence should be addressed.
E-mail: piyasan.p@chula.ac.th

were dissolved in separately water. Aqueous CA solution was prepared and its pH was adjusted to ca. 1 by addition of 35% nitric acid. CA solution was added to the zirconyl nitrate solution at a molar ratio of [Al + Zr:CA] = 3:7. Aluminium nitrate solution was added to the zirconyl citrate complex and finally ethylene glycol was added. The pH of the solution was adjusted to 7, by addition of 35% ammonium hydroxide, to form an alumina gel [18]. The resulting solution was heated under vacuum in a rotary evaporator at 90–100 °C until it became viscous and yellow. After the vacuum was removed, the solution became black and gel-like. This material was removed from the system, dried at 100 °C overnight and calcined in flowing air, with a heating rate of 1 °C/min and final temperature of 500 °C held for 6 h. In the case of pure zirconia, the gel-like material did not appear during the rotary evaporation step, even after many hours, but appeared after the vacuum was removed.

2.2. *Characterisation*

Characterisation of the samples using various analysis techniques was carried out on the calcined samples. The surface area was measured by nitrogen physisorption at 77 K after outgassing at 300 °C. Surface areas were determined by the BET method and pore-size distribution by the BJH method. The crystal structures were characterised by XRD (Siemens D5000) using nickel filtered CuK$_\alpha$ radiation. TPD of CO_2 was used to characterise the basic sites of the oxides. Samples were pre-treated at 400 °C for 1 h in He, then saturated with CO_2 (99.99%) at 35 °C for 3 h. Desorption of CO_2, by heating at 10 °C/min to 400 °C, was measured using a GOW-MAC thermal conductivity detector (TCD). TPD of NH_3 (Micromeritics Autochem 2910) was used to characterise the acid sites. Samples were pre-treated in He at 400 °C for 1 h and saturated with 10%NH_3/He at 100 °C for 2 h. Adsorbed NH_3 was removed by flowing He (10 mL/min) while heating at 10 °C/min to 400 °C and detected by TCD.

2.3. *Catalytic activity*

Catalyst testing was carried out at atmospheric pressure in a quartz fixed-bed reactor. The catalyst sample was treated in air at 400 °C for 1 h prior to the reaction to remove adsorbed H_2O and CO_2. Elimination of 2-propanol was carried out at 150, 200 and 250 °C as in [19,20]. Helium (~12 mL/min) was bubbled through 2-propanol at fixed temperature (~50 °C) to give a concentration of 12-mol% 2-propanol in He flowing through 100 mg of catalyst. Typical space velocities (WHSV) were in the range of 20–200 h^{-1} as in [20]. Reaction products were analysed using a Shimadzu GC-14A gas chromatograph with a flame ionisation detector and a column containing 15%-Carbowax 1000 supported on Chromosorb W. Measurements were taken every 20 min until a steady state was reached, typically after about 2 h. The reaction products were propylene, acetone and diisopropyl ether.

3. Results

3.1. *N_2 adsorption*

The BET surface areas and BJH pore size distributions of the mixed oxides solid powders after calcination for 6 h at 500 °C are given in table 1. The surface areas increased with alumina content. For pure zirconia, most of the pores were macro-sized (>50 nm), while the mixed oxides had pore volumes more evenly distributed between micro-, meso- and macropores. Pure alumina had most of its pore volume in the meso and macro range.

3.2. *XRD analysis*

Crystal phases of the mixed oxides were identified by XRD. Figure 1 shows the XRD patterns of pure zirconia, $Al_{40}Zr_{60}$ and pure alumina after calcination at 1000 °C. The identified crystal structures and crystallite sizes after ignition at 500 °C and calcinations at 800 and 1000 °C calculated using Scherrer's equation are shown in table 2.Calcination of zirconia at 500 °C and above gave mostly tetragonal phase, with the monoclinic phase becoming dominant at 1000 °C. Alumina was amorphous after calcination at 500 °C and changed from θ to α between 800 and 1000 °C. In the mixed oxide sample, no alumina XRD peaks could be detected at any temperature. The sample calcined at 500 °C was completely amorphous while only tetragonal zirconia peaks were detected even at 1000 °C. In all cases, the crystallite sizes increased with increasing calcinations temperature.

Table 1
Surface area and pore size distribution of zirconia, alumina and mixed oxides

Composition (mol%)	BET surface area (g/m^2)	BJH pore size distribution (%)		
		Micro < 2 nm	Meso 2–50 nm	Macro > 50 nm
Zirconia	56	6.2	24.1	69.7
$Al_{25}Zr_{75}$	70	26.4	43.8	29.7
$Al_{40}Zr_{60}$	182	24.5	33.9	41.7
$Al_{75}Zr_{25}$	228	34.2	30.5	35.4
Alumina	319	13.6	44.7	41.7

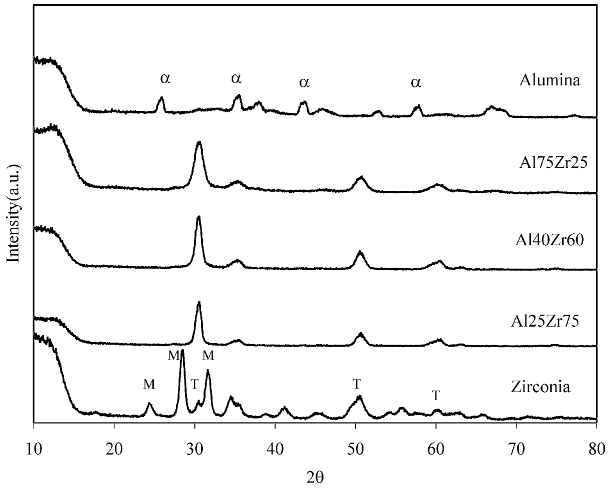

Figure 1. XRD diffraction pattern of zirconia, alumina and zirconia alumina mixed oxide calcined at 1000 °C.

Table 2
Crystal structure and size of zirconia crystals in zirconia, alumina and mixed oxides

Sample	Crystal structure (crystal size, nm)		
	Calcination temperature		
	500 °C	800 °C	1000 °C
Zirconia	T(13)	T(26)	M(31),T
$Al_{25}Zr_{75}$	A	T(13)	T(28)
$Al_{40}Zr_{60}$	A	T(14)	T(19)
$Al_{75}Zr_{25}$	A	A	T(13)
Alumina	A	θ	α

Symbols A, M and T indicate amorphous, monoclinic and tetragonal phases of zirconia (or pure alumina) respectively.
Symbols θ and α indicate theta and alpha phases of alumina respectively.

3.3. CO_2 temperature programmed desorption

Basicity of the catalysts was measured by CO_2 temperature programmed desorption up to 400 °C. Figure 2 shows the CO_2 TPD profiles of all the catalyst samples. In all cases, a single desorption peak was observed around 100–115 °C. The CO_2 desorption temperature of pure zirconia and pure alumina were found to be slightly lower than that of the mixed oxides. The amounts of CO_2 desorbed from the mixed oxides, pure alumina and pure zirconia were calculated by integrating the areas of CO_2 TPD profiles and are reported in table 3.

3.4. NH_3 temperature programmed desorption

Acidity of the catalysts was measured by NH_3-TPD. The NH_3 TPD profiles for all the catalysts are shown in figure 3. None of the materials tested showed distinct NH_3 desorption peaks up to 400 °C. The broad desorption peaks below 200 °C occurred at slightly higher temperature for two of the mixed oxides than for pure alumina or zirconia. This suggests that the acid strength of those mixed oxides is slightly greater than the pure oxides. Table 3 also shows the amounts of NH_3 desorbed from each sample.

3.5. Reaction test

The catalytic activities of the mixed oxide were tested in the elimination reactions of 2-propanol at 150, 200, and 250 °C. The results are given in table 4. At 150 °C,

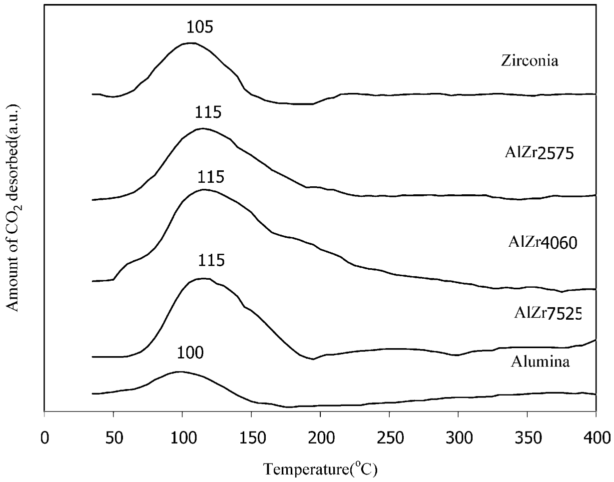

Figure 2. Temperature programmed desorption of CO_2 on mixed oxide, pure zirconia and pure alumina.

the elimination product was almost entirely acetone for all catalysts. At 200 °C, the product distribution depended on the catalyst composition. Catalysts high in alumina content produced mainly acetone, while those high in zirconia produced large amounts of propylene. Traces of diisopropyl ether appeared at this temperature. At higher temperature (250 °C) the product distribution changed again, to favour propylene production over all materials. Catalysts high in alumina also produced significant amounts of diisopropyl ether at this temperature. It should be noted that alumina activated in oxygen can exhibit dehydrogenation activity that may exceed considerably the dehydration selectivity [21]. However, the effect of oxygen pretreatment was not observed in this study (no oxidation reaction) since one would expect changes in selectivity of acetone with increasing reaction time due to consumption of oxygen covering the catalyst surface.

Table 3
Quantities of $CO_2$and NH_3 desorbed from zirconia, alumina and mixed oxides

Sample	CO_2 desorbed (μmol/g)	NH_3 desorbed (μmol/g)
Zirconia	172	202
$Al_{25}Zr_{75}$	279	478
$Al_{40}Zr_{60}$	632	752
$Al_{75}Zr_{25}$	485	830
Alumina	146	69

4. Discussion

The macropore system may occur after removal of organic material polymerised from CA and ethylene glycol in fresh gel. It is suggested that under these preparation conditions, well dispersed alumina and zirconia influencing orientation of alumina and zirconia crystal structure of the mixed oxide. Using this method, tetragonal phase of pure zirconia were obtained after calcination at 500 °C. The tetragonal phase zirconia is thermodynamically stable at a temperature above 1170 °C [22]. However, removal of combustible organic materials at 500 °C during preparation could result in sufficient energy to arrange the zirconia structure in tetragonal form.

Surface properties of pure zirconia, pure alumina and the mixed oxides might be classified into two types by probe molecule adsorption; CO_2 and NH_3 probe molecules. The interaction between CO_2 probe molecule and zirconia or mixed oxides surfaces might be physical adsorption in accordance with a result of Li *et al.* [23] showing desorption of CO_2 physical bonding on zirconia surface is around 100 °C. Desorption temperatures might be improved to be higher after atomically mixing zirconia with alumina. This is probably due to the interaction between aluminium, oxygen and zirconium ions in the mixed oxide increasing the physical strength between surface oxygen and CO_2 probe molecule.

It is known that the reaction pathways of 2-propanol elimination forming dehydration and dehydrogenation products occur on different nature and strength of acid–base sites [20]. Different mechanisms have been derived

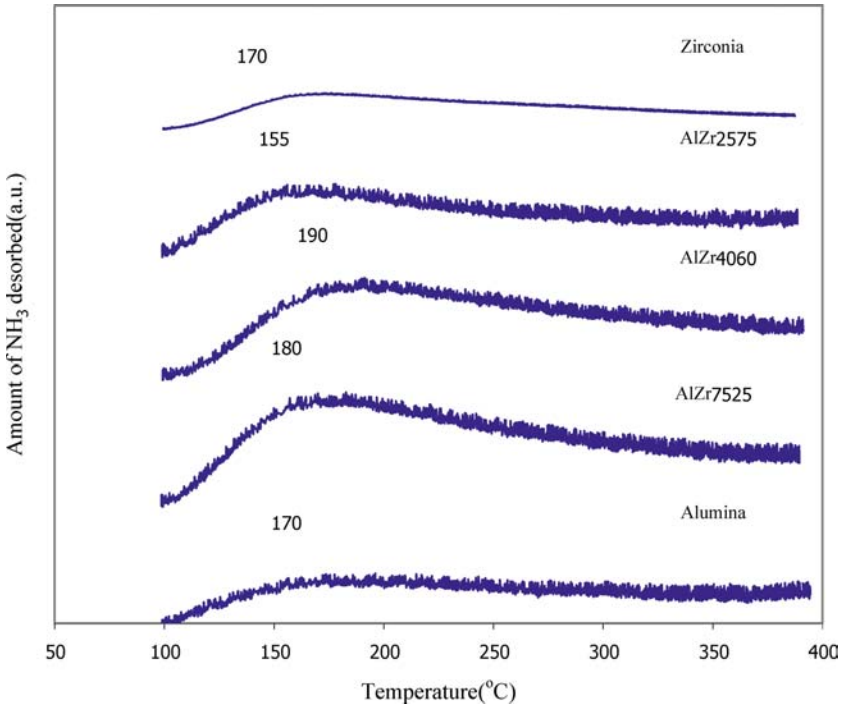

Figure 3. Temperature programmed desorption of NH_3 on mixed oxide, pure zirconia and pure alumina.

Table 4
Catalyst activity and selectivity during elimination of 2-propanol

Sample	T = 150 °C				T = 200 °C				T = 250 °C			
	% Conversion	S_P	S_A (%)	S_{DIP}	% Conversion	S_P	S_A (%)	S_{DIP}	% Conversion	S_P	S_A(%)	S_{DIP}
Alumina	3.5	2.0	98.0	0.0	9.8	1.6	98.1	0.3	36.6	66.3	24.1	9.5
$Al_{75}Zr_{25}$	5.5	1.3	98.7	0.0	2.5	6.3	92.6	1.1	6.9	66.6	28.7	4.6
$Al_{40}Zr_{60}$	0.3	10.2	89.8	0.0	1.0	7.7	92.3	0.0	10.7	48.3	48.8	2.9
$Al_{25}Zr_{75}$	2.2	2.0	98.0	0.0	1.3	27.5	71.7	0.8	7.5	64.3	34.5	1.2
Zirconia	1.0	8.9	91.1	0.0	4.4	89.2	10.2	0.6	7.5	75.2	24.5	0.3

based on individual transition states including E_1, E_2, and E_{1cB} [20,25]. E_1 mechanism requires strong acidic catalysts to form carbenium ions by abstraction of OH-group. The carbenium ions are rearranged via isomerisation and abstracted hydrogen resulting in different kind of alkenes [25].

In this study, the NH_3 temperature programmed desorption results exhibited a single peak below 200 °C suggesting that the acidic strength was probably unable to abstract OH groups. The E_1 mechanism then can be excluded. For E_2 mechanism, reaction occurs on dual acid–base sites to simultaneously eliminate a proton and hydroxyl group producing the main product alkene whereas for E_{1cB} mechanism, strong basic sites are required in order to firstly detach β hydrogen and then eliminate hydroxyl group [25].

Recently, Díez *et al.* [20,26] propose a mechanism slightly different from E_{1cB} mechanism in which reaction takes place via acid–base sites of imbalanced strength. Adsorption of OH group occurs on weak acid–base sites to form a surface propoxide intermediate. The most acidic hydrogen of alcohol is attacked by strong base site (the surface oxygen), in contrast, the Lewis acid site (the surface cation) attacks the oxygen of alcohol resulting in rupture of hydroxyl groups. Two pathways were proposed after forming propoxide on the surface: (a) dehydration of 2-propanol where acetone is a result of abstraction α-hydrogen and (b) dehydrogenation of 2-propanol producing propylene by detaching β-hydrogen. The products of the E_{1cB} mechanism could be either propylene or acetone or both depending on the strength of base site. However, the base site detaching β-hydrogen is stronger than the one detaching α-hydrogen. Waugh *et al.* [26,27] found that the activation energy of α-hydrogen abstraction is lower than the activation energy of β-hydrogen abstraction.

Generally, elimination of 2-propanol on alumina produces propylene as the main product via E_2 mechanism due to amphoteric properties of alumina [19, 28]. Dominuguez *et al.* [19] showed that γ-alumina gave propylene selectivity more than 80% in a range of reaction temperature 180–240 °C. However, in this study we observed that most of the propanol elimination products over the Pechini alumina were more than 90% acetone. Disordered structure of the Pechini amorphous alumina could result in an imbalanced strength of acid–base sites and the reaction pathway might occur via E_{1cB} proposed by Díez *et al.* The weak physically adsorbing CO_2 site of alumina as shown by the low temperature CO_2 desorption peak in figure 2 could bring about abstraction of α-hydrogen mostly resulting in acetone formation. This might be representative of very poor basicity of alumina surface.

Similar to the pure alumina, the Pechini alumina–zirconia mixed oxides converted to propanol towards acetone with more than 70% selectivity at 150 and 200 °C. Increasing zirconia content in the mixed oxides resulted in a slight decrease in acetone and increase in propylene selectivity at 200 °C. The propylene formation may be ascribed to zirconia. The E_{1cB} mechanism appeared to dominate over the alumina–zirconia mixed oxides. Although the CO_2 desorption peaks of the mixed oxides shifted towards 115 °C, the strength of basicity would not be very effective to abstract β-hydrogen. Increasing propylene selectivity over the alumina–zirconia mixed oxides was probably affected by dual acid–base property of zirconia via the E_2 mechanism. This is in a good agreement with the work reported by Tanabe [29], in which 2-propanol elimination on zirconia catalysts proceed by acid–base site bifunctional catalysis. The orientation of these sites plays an importance role in governing the reaction [30]. However, the orientation of alumina–zirconia mixed oxides structure would be undisciplined resulting in a decrease in acid–base bifunctional property. Therefore, the E_2 mechanism would not dominate over the alumina–zirconia mixed oxides.

Conversion of propanol towards propylene over tetragonal zirconia was observed with more than 80% selectivity at 200 °C. The well-ordered structure of tetragonal zirconia exhibited high selectivity of propylene via the dominant E_2 mechanism. In contrast, partly imperfect crystal of tetragonal zirconia could result in imbalanced acid–base site leading to acetone formation via the E_{1cB} mechanism.

5. Conclusions

The alumina–zirconia mixed oxides produced by the modified Pechini method resulted in combination of aluminium and zirconium atoms. Due to good dispersion of aluminium and zirconium ions, the mixed oxides present only amorphous form. Apparently, the interaction between Al, Zr, and O in the mixed oxides resulted in higher physical strength of CO_2 adsorption. The modified acidity was, however, ambiguous because all the catalyst samples exhibited low acidity. The imbalance strength of acid–base site due to the imperfect crystal structure of all the catalysts resulted in higher acetone formation via E_{1cB} mechanism. However, 90% propylene selectivity was obtained on pure zirconia prepared by the modified Pechini method and 200 °C reaction temperature.

Acknowledgments

The authors would like to thank the Cooperative Research Network, Thai Ministry of Education, the Thailand Research Fund, the University of New South Wales and CSIRO for financial support. The authors also thank Mr Praharso, Ms Sarah Watson, Mr Richard Burgess and Mr John Starling and Dr Manh Hoang for their support.

References

[1] G. Ertl, H. Knözinger and J. Weitkamp, *Handbook of Heterogeneous Catalysis* (Wiley-VCH, City, 1997).
[2] J.C. Debsikdar, J. Non-Cryst. Solids 86 (1986) 231.
[3] R. Guinebretière, A. Dauger, A. Lecomte and H. Vesteghem, J. Non-Cryst. Solids 147&148 (1992) 542.
[4] J. Livage, F. Beteille, C. Roux, M. Chatry and P. Davidson, Acta mater. 46 (1998) 743.
[5] C. Stöcker and J. Baiker A., Non-Cryst. Solids 223 (1998) 165.
[6] M.M. Pineda, S. Castillo, T. López, R. Gómez, Cordero-Borboa and O. Novaro, Appl. Catal. B: Environ. 21 (1999) 79.
[7] J.L. Lakshmi, T.R.B. Jones, M. Gurgi and J.M. Miller, J. Mol. Catal. A: Chem. 152 (2000) 99.
[8] D.D. Jayaseelan, D.A. Rani, T. Nishikawa, H. Awaji and F.D. Gnanam, J. Euro. Ceram. Soc. 20 (2000) 267.
[9] A.C. Geiculescu and H.J. Rack, J. Non-Crytal. Solids 289 (2001) 53.
[10] Y. Hao, J. Li, X. Yang, X. Wang and L. Lu, Mat. Sci. Eng. A 367 (2004) 243.
[11] M. Ishii, M. Kakihana, K. Ishii, Y. Ikuma and M. Yoshimura, J. Mat. Res. Soc. 11(6) (1996) 1410.
[12] M. Kakihana, S. Kato, M. Yashima and M. Yoshimura, J. Alloys Comp. 280 (1998) 125.
[13] E.N.S. Muccillo, E.C.C. Souza and R. Muccillo, J. Alloys Comp. 344 (2002) 175.
[14] M.P. Pechini, Patent, 11 July (1967) 3,330,697.
[15] C.L. Robert, F. Ansart, C. Deloget, M. Gaudon and A. Rousset, Ceram. Int. 29 (2003) 151.
[16] Y.M. Kong, C.J. Bae, S.H. Lee, H.W. Kim and H.E. Kim, Biomaterials 26 (2005) 509.
[17] I.I. Abu, D.D. Das, H.K. Mishra and A.K. Dalai, J. Colloid Interface Sci. 267 (2003) 382.
[18] R. Mezei and K. Sinkó, Colloid Polym. Sci. 274 (1996) 1054.
[19] J.M. Dominguez, J.L. Hernandez and G. Sandoval, Appl. Cata. A: Gen. 197 (2000) 119.
[20] V.K. Díez, C.R. Apesteguía and J.I. Di Cosimo, J. Catal. 215 (2003) 220.
[21] B.H. Davis, J. Catal. 26 (1972) 348.
[23] P.D.L. Mercera, J.G. van Ommen, E.B.M. Doesburg, A.J. Burggraaf and J.R.H. Ross, Appl. Catal. 71 (1991) 363.
[23] Y. Li, D. He, Z. Cheng, C. Zu, J. Le and Q. Zhu, J. Mol. Catal. A: Chem. 175 (2001) 267.
[24] A. Davydov, *Molecular Spectroscopy of Oxide Catalyst Surfaces* (John Wiley & Sons, England, 2003).
[25] K. Tanabe, M. Misono, Y. Ono and H. Hattari, *New Solid Acids and Bases Their Catalyst Properties* (Kodansha, Tokyo, 1989).
[26] V.K. Díez, C.R. Apesteguía and J.I. Di Cosimo, Catal. Today 63 (2000) 53.
[27] K.C. Waugh, M. Bowker, R.W. Petts, H.D. Vanderwell and J. O'Malley, Appl. Catal. 25 (1986) 121.
[28] A. Gervasini, J. Fenyvesi and A. Auroux, Catal. Lett. 43 (1997) 219.
[29] K. Tanabe, Mat. Chem. Phys. 13 (1985) 347.
[30] S. Chokkaram and B.H. Davis, J. Mol. Catal. A: Chem. 118 (1997) 89.